Journal of Engineering and Applied Science

RESEARCH Open Access

Effects of welding parameters optimization on the tensile performance of friction stir welded AA3103 Al alloy

Ganesh Jagannath Pagar[1,2] and Gajanan N. Shelke[3*]

*Correspondence:
Gajanan N. Shelke
gnshelke@gmail.com
[1]Present address: Department of Mechanical Engineering, MET BKC's Institute of Engineering, Nashik, Maharashtra 422003, India
[2]Savitribai Phule Pune University, Pune, Maharashtra, India
[3]Present address: Department of Mechanical Engineering, Sandip Foundation's Sandip Institute of Engineering & Management, Nashik, Maharashtra 422213, India

Abstract

Friction Stir Welding (FSW) is a reliable solid-state joining technique for aluminium alloys, where conventional fusion welding often causes porosity, solidification cracking, and excessive heat-affected softening. The present study investigates the influence of tool pin geometry, shoulder-to-pin diameter ratio, rotational speed, and welding speed on the mechanical performance of friction stir welded AA3103 aluminium alloy. Twenty-seven experimental trials were conducted using a Taguchi L9 orthogonal array, repeated for three tool pin profiles: circular, square, and triangular. Three shoulder-to-pin diameter ratios (D/d = 3, 4, 5), rotational speeds (355, 710, and 1400 RPM), and welding speeds (20, 40, and 80 mm/min) were considered. Mechanical testing was performed according to ASTM E8 to determine yield strength, ultimate tensile strength (UTS), and percentage elongation. Statistical evaluation using Signal-to-Noise ratio and General Linear Model based ANOVA revealed that the shoulder-to-pin diameter ratio significantly influences UTS and YS at a 95% confidence level ($p < 0.05$). The maximum UTS of 174.37 MPa was achieved using a square pin at D/d = 3, 355 RPM, and 20 mm/min, while maximum elongation of 26% was obtained with a triangular pin at higher rotational speed. Regression models showed acceptable predictive accuracy for process optimization.

Keywords Friction Stir Welding, AA3103, Taguchi Optimization, ANOVA, Tensile Properties

Introduction

Aluminium alloys play a significant role in modern engineering applications such as transportation, marine structures, construction systems, and packaging industries due to their high specific strength, excellent corrosion resistance, and good formability characteristics [1]. Among these alloys, AA3103, an aluminium–manganese alloy belonging to the 3xxx series, is widely used for sheet-based applications because of its balanced combination of moderate strength, high ductility, and superior workability. These characteristics make AA3103 particularly suitable for lightweight structures where reliable joining and structural integrity are essential. However, achieving

high-quality joints in AA3103 using conventional fusion welding processes remains challenging. Fusion welding involves localized melting and solidification, which often leads to distortion, porosity formation, and deterioration in mechanical properties of the welded joints [1, 2]. To overcome these limitations, Friction Stir Welding (FSW) has emerged as an efficient solid-state joining technique. In this process, a rotating non-consumable tool consisting of a shoulder and a protruding pin is inserted into the joint interface and moved along the weld line. The frictional heat generated between the tool and workpiece, combined with severe plastic deformation, softens the material below the melting temperature, resulting in solid-state bonding. Since melting is avoided, FSW generally produces superior mechanical properties, improved dimensional stability, and reduced welding defects compared to conventional fusion welding techniques [1, 3–6]. Previous studies have demonstrated that FSW significantly improves microstructural refinement and mechanical performance in aluminium alloys, making it an attractive joining method for industrial applications [7–10]. The tensile performance of friction stir welded joints is strongly influenced by tool design and process parameters. Important factors include tool pin profile, shoulder-to-pin diameter ratio (D/d), rotational speed, welding speed, and the material flow behavior during welding [2, 11]. The tool pin geometry plays a crucial role in determining the intensity of material stirring and plastic flow characteristics, which directly affect weld quality and joint strength. Meanwhile, the shoulder diameter controls frictional heat generation and forging pressure applied during welding. Rotational speed governs heat input and plasticization rate, whereas welding speed determines heat input per unit length and tool-material interaction time. Improper combinations of these parameters may result in insufficient material flow, tunnel defects, excessive flash formation, or grain coarsening, ultimately reducing tensile performance and ductility. Therefore, systematic optimization of process parameters is essential to achieve high-quality joints with improved mechanical performance [2, 11–13]. Although numerous studies have investigated the influence of tool geometry and process parameters on different aluminium alloys, comprehensive statistical evaluation for AA3103 alloy remains limited. In particular, the contribution of shoulder-to-pin diameter ratio (D/d) and tool pin profile on tensile properties of AA3103 has not been extensively quantified using structured experimental design and statistical modeling approaches. Many previous studies primarily focused on experimental observations without employing rigorous statistical validation techniques such as ANOVA and regression modeling to identify dominant parameters with confidence [1, 2, 14].

In this context, the present investigation aims to perform a systematic experimental and statistical evaluation of friction stir welded AA3103 joints. Three different tool pin profiles are selected to examine their influence on tensile performance. A Taguchi L9 orthogonal array is employed to design the experimental matrix, allowing efficient analysis of multiple parameters at three levels. The statistical significance of process parameters is evaluated using Signal-to-Noise ratio analysis and General Linear Model (GLM)-based ANOVA. Furthermore, regression models are developed to predict ultimate tensile strength, yield strength, and percentage elongation within the experimental range. The objective of this study is to establish a statistically validated parameter hierarchy and determine optimal welding conditions that enhance both strength and

ductility, thereby providing a reliable framework for industrial application of friction stir welding of AA3103 alloy.

Experimental set-up

The experimental investigation was performed using a conventional vertical milling machine modified for friction stir welding operations [15]. A specially designed rigid clamping fixture was mounted on the machine table to securely hold the aluminium plates during the welding process [16]. The fixture ensured accurate alignment of the plates along the welding direction and minimized vibration during tool movement, thereby improving weld stability and repeatability [16]. The non-consumable rotating tool was mounted in the machine spindle using a collet system to maintain proper concentricity and stable rotational motion during welding [15]. The spindle rotational speeds were selected according to the machine speed selector chart, and welding was carried out in position-controlled mode by maintaining a constant travel speed along the joint interface [17]. This approach ensured uniform heat generation and consistent material flow during welding. After completion of welding, visual inspection of the weld surface was performed to evaluate surface quality and flash formation. The welds exhibited uniform surface appearance and consistent flash along the weld line, indicating adequate material plasticization and proper consolidation under the selected process conditions [4–7, 17].

Base material

Commercial AA3103 aluminium alloy plates were selected as the base material for the present investigation [18]. AA3103 belongs to the aluminium–manganese (3xxx) series and is widely used in sheet fabrication industries due to its balanced combination of moderate tensile strength, good corrosion resistance, and excellent formability [18, 19]. These characteristics make it suitable for evaluating the mechanical performance of friction stir welded joints under varying process parameters [20]. The chemical composition of the base material is presented in Table 1 [18]. Aluminium constitutes the major portion of the alloy, with manganese as the primary alloying element responsible for strengthening [19]. Minor elements such as magnesium, iron, silicon, copper, zinc, and titanium are present within controlled limits as per commercial standards [18]. The composition ensures stable mechanical behavior and consistent response during solid-state joining operations [20].

Tool design and geometry

The friction stir welding tools were fabricated from high-strength tool steel to withstand elevated temperatures and severe frictional conditions encountered during welding [21]. The chemical composition of the tool material is presented in Table 2. The presence of chromium, molybdenum, and vanadium improves wear resistance and thermal stability, thereby maintaining dimensional integrity during repeated welding

Table 1 Chemical composition of base metal AA3103

Al (%)	Mn (%)	Mg (%)	Fe (%)	Si (%)	Cu (%)	Zn (%)	Ti (%)	Others (each %)	Al (%)
Balance (~96–98)	1.0 – 1.5	0.8 – 1.3	≤ 0.7	≤ 0.6	≤ 0.1	≤ 0.1	≤ 0.1	≤ 0.05	Balance (~96–98)

Table 2 Chemical composition of H13 tool material

Fe (%)	C (%)	Cr (%)	Mo (%)	V (%)	Si (%)	Mn (%)	*P* (%)	S (%)	Fe (%)
Balance	0.32 – 0.45	4.75 – 5.50	1.10 – 1.75	0.80 – 1.20	0.80 – 1.20	0.20 – 0.50	≤ 0.03	≤ 0.03	Balance

Fig. 1 Friction Stir Welding (FSW) tools with different pin profiles – square, circular, and triangular

trials [4, 21, 22]. Three different non-consumable tool pin profiles were designed to evaluate the influence of geometry on tensile performance: circular pin, square pin, and triangular pin [23]. The variation in pin geometry alters material flow behavior and stirring action, which directly influences weld quality and mechanical performance [5, 23, 24]. To systematically examine the shoulder influence, three different shoulder-to-pin diameter ratios (D/d) were selected: 3, 4, and 5 [24]. These correspond to shoulder diameters of 15 mm, 20 mm, and 25 mm, respectively, while maintaining a constant pin diameter of 5 mm. Maintaining a constant pin diameter ensured that the effect of shoulder diameter variation could be isolated and statistically evaluated without introducing additional geometric variables [6, 23].

The fabricated tools were mounted using a precision collet system to ensure axial alignment and minimize eccentricity [22]. The experimental set-up, including the vertical milling machine, fixture assembly, tool mounting system, and welded specimen configuration, is illustrated in Fig. 1.

The friction stir welding experiments were conducted using a conventional vertical milling machine adapted for solid-state joining operations [25]. The machine spindle provided controlled rotational motion to the non-consumable FSW tool, and multiple selectable spindle speeds enabled precise control of rotational speed during experimentation [25, 26]. The rigid structure of the vertical milling machine minimized vibration and ensured stable tool engagement throughout the welding process [4, 26]. A specially designed FSW fixture was fabricated to securely clamp the aluminium plates on the machine Table [27]. The fixture consisted of a flat base plate, rigid clamping elements, bolts, and support blocks to prevent lateral and vertical movement during welding [27]. Proper alignment of the plates was maintained along the welding direction to ensure consistent tool travel and uniform joint formation [28]. The clamping system was also designed to withstand the axial force exerted by the rotating tool, thereby preventing plate separation during processing [5, 27].

The FSW tool was mounted in the machine spindle using a precision collet system to ensure concentricity and minimize run-out [28]. This arrangement provided firm gripping of the tool shank and maintained axial stability under combined rotational and axial loading conditions [28]. The tool consisted of a shoulder and a protruding pin to generate frictional heat and mechanical stirring action during welding [25]. Welding

was performed in position-controlled mode, where the rotating tool was plunged into the abutting edges of the aluminium plates and traversed along the joint line at predetermined welding speeds [26]. During welding, visible flash formation was observed along the weld surface, indicating adequate plastic deformation and material consolidation under the selected process conditions [6–8, 29]. The welded plates were visually inspected to ensure uniform surface appearance and absence of major surface defects [29]. Spindle speeds were selected according to the machine's speed chart, and welding speed was controlled through the table feed mechanism [26]. The combination of controlled rotational speed, stable axial force application, and rigid clamping ensured repeatability of experimental trials across different parameter combinations [29] (Fig. 2).

Design of experiment

Figure 3 presents the fishbone diagram developed to identify the factors influencing welding quality in the friction stir welding process [30–32]. The diagram categorizes parameters into major groups such as tool shoulder design, pin characteristics, clamping conditions, and process variables [30, 33, 34]. Elements including shoulder geometry, shoulder-to-pin diameter ratio, pin profile, rotational speed, traverse speed, clamping force, and clamping geometry are identified as key contributors to joint performance [33–35]. This structured representation illustrates the cause–effect relationship between process parameters and welding quality, facilitating the selection of significant variables for experimental investigation [4, 31, 36, 37].

The process parameters considered are summarized below [34, 38, 39] (Table 3):

To quantitatively evaluate the influence of selected parameters, a Taguchi L9 orthogonal array with three levels for each factor was adopted [40, 41]. The primary variables considered were tool pin profile (circular, square, triangular), shoulder-to-pin diameter ratio (3, 4, 5), rotational speed (355, 710, 1400 RPM), and welding speed (20, 40, 80

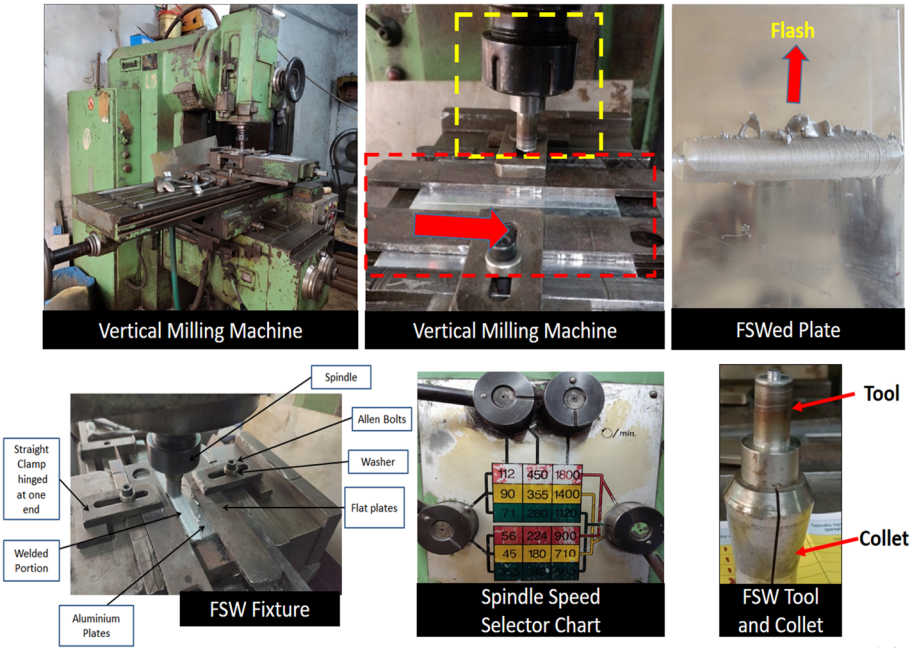

Fig. 2 Friction stir welding setup

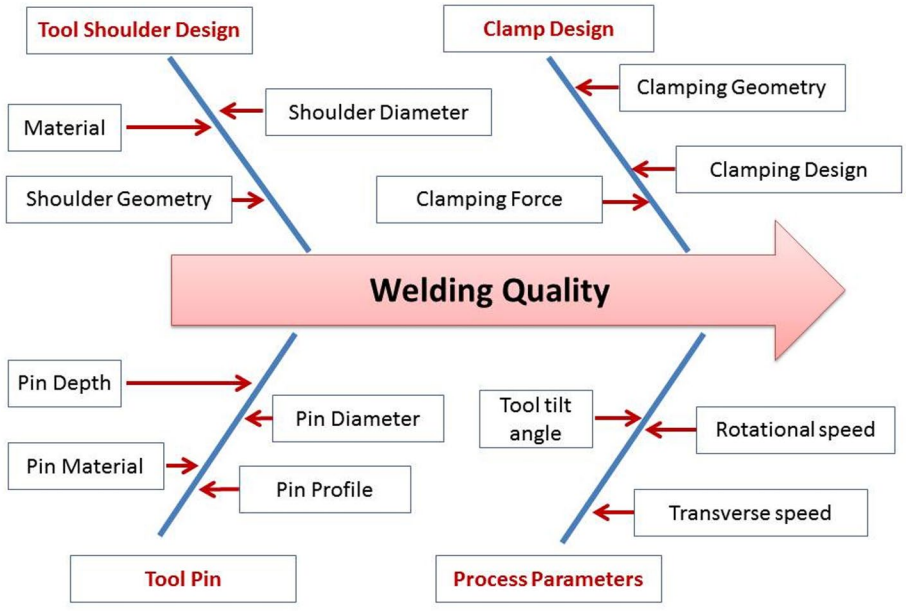

Fig. 3 Fishbone diagram for welding parameters

Table 3 Parameters & Levels for DOE

Parameter	Levels
Tool Pin Profile	Circular, Square, Triangular
Shoulder/Pin Ratio	3, 4, 5
Rotational Speed	355, 710, 1400 RPM
Welding Speed	20, 40, 80 mm/min

mm/min). The L9 design was executed three times corresponding to the three pin profiles, resulting in a total of 27 experimental trials [40]. This approach ensured balanced experimentation, reduced the number of required runs, and enabled reliable statistical evaluation of parameter significance [13, 14, 41].

The experimental matrix presented in Table 4 was developed using a Taguchi L9 orthogonal array to evaluate the combined influence of tool pin profile, shoulder-to-pin diameter ratio (D/d), rotational speed (RPM), and welding speed (WS) on the tensile performance of friction stir welded AA3103 joints. Three tool pin geometries—square (PS), circular (PC), and triangular (PT)—were investigated independently under identical three-level parameter combinations (D/d = 3, 4, 5; RPM = 355, 710, 1400; WS = 20, 40, 80 mm/min), resulting in 27 experimental trials. This design ensured balanced experimentation and reliable statistical comparison of parameter effects [13, 40, 41].

The response variables recorded were yield strength (YS), ultimate tensile strength (UTS), and percentage elongation (%E). The results show noticeable variation in tensile properties across parameter combinations, indicating the sensitivity of mechanical performance to process conditions. Tensile specimens were prepared according to ASTM E8 standards and tested using a calibrated Universal Testing Machine under displacement-controlled loading. All specimens fractured within the gauge length, as shown in Fig. 4, confirming the reliability of the tensile data and proper joint formation under the selected experimental conditions [4, 14].

Table 4 Design of experiment according to Taguchi L9 for three tool pin profile (square, circular and triangular) and corresponding response values

Expt No.	Tool Pin Profile	D/d	RPM	WS	YS (MPa)	UTS (MPa)	% E
1	PS	3	355	20	139.07	174.37	22
2	PS	3	710	40	121.27	161.34	21.2
3	PS	3	1400	80	129.05	163.95	20.8
4	PS	4	355	40	107.37	137.82	20.4
5	PS	4	710	80	118.65	153.33	20.4
6	PS	4	1400	20	104.72	132.25	24.8
7	PS	5	355	80	60.98	101.63	22
8	PS	5	710	20	106.91	147.78	24.4
9	PS	5	1400	40	103.2	126.01	22
10	PC	3	355	20	124.6	162.25	22.4
11	PC	3	710	40	118.7	156.84	24.8
12	PC	3	1400	80	122	159.78	22
13	PC	4	355	40	101.26	130.5	22.8
14	PC	4	710	80	97.96	101.59	22.8
15	PC	4	1400	20	92.51	101.98	25.2
16	PC	5	355	80	105.8	132.25	22
17	PC	5	710	20	104.94	135.08	20.8
18	PC	5	1400	40	108.02	140.49	22
19	PT	3	355	20	83.93	102.88	22.8
20	PT	3	710	40	113.2	146.74	22
21	PT	3	1400	80	117.75	154.02	24.8
22	PT	4	355	40	105.02	137.26	22.4
23	PT	4	710	80	108.78	143.59	23.2
24	PT	4	1400	20	107.42	137.11	22.8
25	PT	5	355	80	106.51	132.87	24.8
26	PT	5	710	20	105.6	135.92	21.2
27	PT	5	1400	40	105.37	133.72	26

Results and discussion

Signal-to-noise ratios (larger-the-better) for UTS, YS and % elongation

The consolidated Signal-to-Noise (S/N) response table quantitatively evaluates the influence of process parameters on ultimate tensile strength (UTS), yield strength (YS), and percentage elongation based on the larger-the-better criterion. For UTS, the shoulder-to-pin diameter ratio (D/d) exhibits the highest delta value of 1.40, ranking first, with the maximum S/N ratio of 43.64 observed at Level 1 (D/d = 3). The tool pin profile ranks second with a delta value of 0.55, followed by rotational speed ($\Delta = 0.54$) and welding speed ($\Delta = 0.38$), indicating comparatively lower influence on tensile strength. A similar trend is observed for yield strength, where D/d again shows the highest influence with a delta value of 1.47 and maximum S/N ratio of 41.43 at Level 1. Rotational speed ranks second for YS with $\Delta = 0.73$, while welding speed ($\Delta = 0.29$) and tool pin profile ($\Delta = 0.19$) demonstrate relatively smaller statistical contributions.

In contrast, percentage elongation is primarily influenced by the tool pin profile, which shows the highest delta value of 0.51 and maximum S/N ratio of 27.34 at Level 3. Rotational speed ranks second with $\Delta = 0.40$, whereas welding speed ($\Delta = 0.15$) and D/d ($\Delta = 0.09$) exhibit comparatively minor effects. These results indicate that strength-related responses (UTS and YS) are predominantly governed by the shoulder-to-pin diameter ratio, while ductility (% elongation) is more sensitive to tool pin

Fig. 4 Fractured tensile specimens of friction stir welded AA3103 joints after ASTM E8 testing

geometry. This establishes a clear statistical hierarchy of parameters for optimizing mechanical performance in friction stir welded AA3103 joints (Fig. 5) (Tables 5).

Analysis of variance (ANOVA) test for tensile strength

The General Linear Model (GLM)-based ANOVA provides a statistical evaluation of the contribution of each process parameter to the tensile performance of friction stir welded AA3103 joints. For ultimate tensile strength (UTS), the shoulder-to-pin diameter ratio (D/d) shows a statistically significant influence with an F-value of 4.28 and a p-value of 0.030, which is below the 0.05 significance level at 95% confidence. This indicates that variations in D/d produce a measurable effect on tensile strength. In contrast, tool pin profile (F = 0.61, $p = 0.554$), rotational speed (F = 0.39, $p = 0.682$), and welding speed (F = 0.14, $p = 0.871$) exhibit p-values greater than 0.05, indicating statistically insignificant contributions to UTS within the selected parameter range. The higher adjusted sum of squares for D/d (3015.9) compared to other parameters further confirms its dominant influence.

A similar trend is observed for yield strength (YS), where D/d again emerges as the only statistically significant parameter (F = 3.92, $p = 0.039$). The adjusted sum of squares for D/d (1610.73) is considerably higher than those for tool pin profile (79.56), rotational speed (255.35), and welding speed (16.54), indicating that most of the variation in YS is associated with changes in shoulder-to-pin ratio. The non-significant p-values for tool pin profile (0.825), rotational speed (0.548), and welding speed (0.961) further confirm their limited influence on yield strength. These results demonstrate consistency between UTS and YS, indicating that strength characteristics are primarily governed by geometric and heat-input-related parameters.

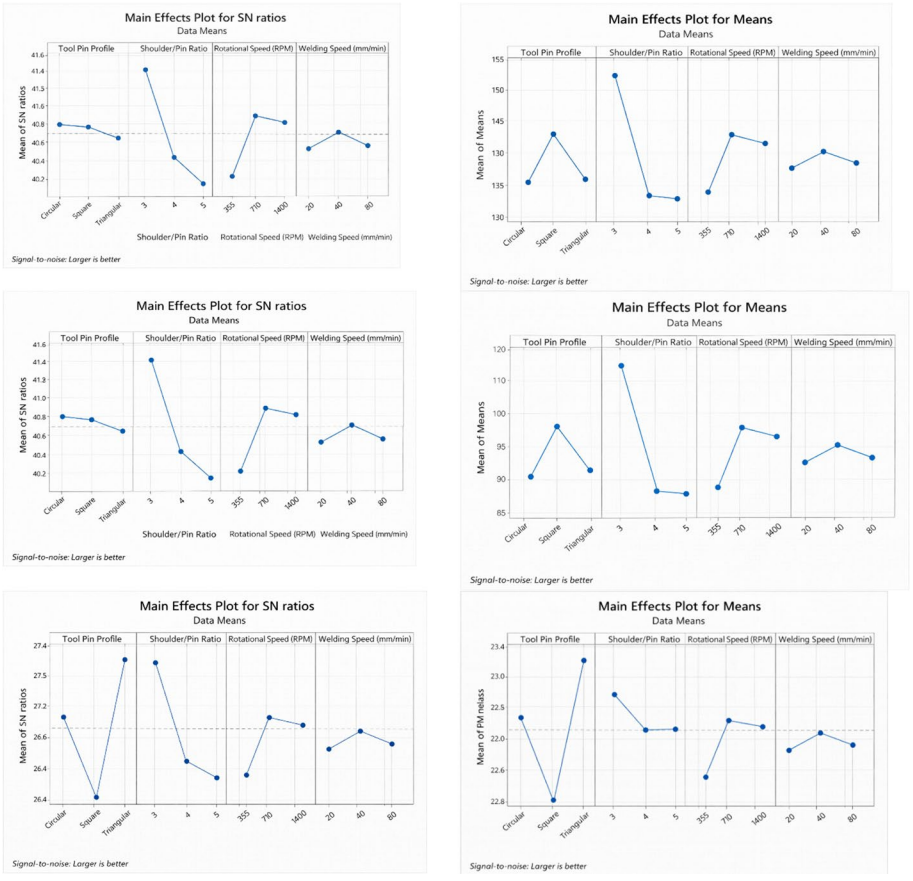

Fig. 5 Signal to noise ratios and main effect plot (Means) for UTS, YS & % E (Using Minitab®). **a** Signal to Noise Ratios for UTS, YS & % E. **b** Main effect plot, (Means) for UTS, YS & %E

Table 5 Response sheet for Signal-to-Noise Ratios (Larger-the-Better) for UTS, YS and % Elongation

Factor	Level	UTS (S/*N*)	YS (S/*N*)	%E (S/*N*)
Tool Pin Profile	1	42.53	40.66	27.13
	2	43.08	40.65	26.83
	3	42.62	40.47	27.34
	Delta	0.55	0.19	0.51
	Rank	2	4	1
Shoulder/Pin Ratio (D/d)	1	43.64	41.43	27.04
	2	42.24	40.39	27.12
	3	42.35	39.96	27.14
	Delta	1.4	1.47	0.09
	Rank	1	1	4
Rotational Speed (RPM)	1	42.46	40.13	26.99
	2	43.01	40.86	26.95
	3	42.77	40.79	27.35
	Delta	0.54	0.73	0.4
	Rank	3	2	2
Welding Speed (WS)	1	42.59	40.56	27.19
	2	42.97	40.75	27.07
	3	42.68	40.46	27.04
	Delta	0.38	0.29	0.15
	Rank	4	3	3

For percentage elongation, ANOVA results show that none of the parameters are statistically significant at the 95% confidence level. Tool pin profile (F = 1.50, $p = 0.250$), rotational speed (F = 1.17, $p = 0.332$), shoulder-to-pin ratio (F = 0.07, $p = 0.934$), and welding speed (F = 0.15, $p = 0.864$) all exhibit p-values greater than 0.05. The relatively low F-values and adjusted sum of squares suggest that elongation variability is influenced by combined parameter interactions or experimental variation rather than a single dominant factor. The error mean square values of 351.92 for UTS, 205.215 for YS, and 2.6864 for percentage elongation indicate acceptable experimental variability and confirm the reliability of the dataset. Overall, the statistical analysis indicates that strength characteristics (UTS and YS) are significantly influenced by shoulder-to-pin diameter ratio, whereas ductility remains statistically insensitive to individual parameter variations within the investigated range (Table 6).

Regression equation

The developed regression equations quantitatively describe the relationship between welding parameters and mechanical responses within the investigated experimental domain. For ultimate tensile strength (UTS), the intercept value of 138.64 MPa represents the overall mean response. Positive coefficients such as + 14.93 for SPR3 and + 3.83 for RPM710 indicate an increase in tensile strength at these parameter levels compared to the reference condition. Conversely, negative coefficients including – 8.04 for SPR4 and – 3.99 for RPM355 indicate a reduction in tensile strength contribution.

A similar trend is observed for yield strength (YS), where SPR3 shows a strong positive coefficient (+ 10.67), confirming the significant influence of a lower shoulder-to-pin diameter ratio on strength improvement. In contrast, the regression model for percentage elongation exhibits relatively smaller coefficient values, indicating lower sensitivity of ductility to individual parameter variations. Among these, RPM1400 (+ 0.681) shows a positive contribution toward elongation.

Table 6 ANOVA results for tensile properties (UTS, YS, and % Elongation)

Response	Source	DF	Adj SS	Adj MS	F-Value	*P*-Value
UTS (MPa)	Tool Pin Profile	2	429	214.49	0.61	0.554
	Shoulder/Pin Ratio	2	3015.9	1507.94	4.28	0.03
	Rotational Speed	2	275.6	137.79	0.39	0.682
	Welding Speed	2	97.6	48.82	0.14	0.871
	Error	18	6334.5	351.92	–	–
	Total	26	10152.6	–	–	–
YS (MPa)	Tool Pin Profile	2	79.56	39.78	0.19	0.825
	Shoulder/Pin Ratio	2	1610.73	805.364	3.92	0.039
	Rotational Speed	2	255.35	127.675	0.62	0.548
	Welding Speed	2	16.54	8.271	0.04	0.961
	Error	18	3693.88	205.215	–	–
	Total	26	5656.06	–	–	–
% Elongation	Tool Pin Profile	2	8.0474	4.0237	1.5	0.25
	Shoulder/Pin Ratio	2	0.3674	0.1837	0.07	0.934
	Rotational Speed	2	6.3052	3.1526	1.17	0.332
	Welding Speed	2	0.7941	0.397	0.15	0.864
	Error	18	48.3556	2.6864	–	–
	Total	26	63.8696	–	–	–

Overall, the regression equations provide predictive capability within the selected parameter range and quantify the directional influence of each parameter level on strength and ductility responses.

Regression Equation for Ultimate Tensile Strength (MPa) is

$$\begin{aligned} UTS\,(MPa) = {} & 138.64 - 3.00\,PC + 5.63\,PS - 2.63\,PT + 14.93\,SPR3 \\ & - 8.04\,SPR4 - 6.89\,SPR5 - 3.99\,RPM355 + 3.83\,RPM710 \\ & + 0.17\,RPM1400 - 2.02\,WS20 + 2.55\,WS40 - 0.53\,WS80 \end{aligned}$$

Regression Equation for Yield Stress (MPa) is

$$\begin{aligned} Yield\ Stress\ (MPa) = {} & 108.17 + 0.25\ PC + 1.97\ PS - 2.22\ PT + 10.67\ SPR3 \\ & - 7.36\ SPR4 - 3.32\ SPR5 - 4.33\ RPM355 + 2.50\ RPM710 \\ & + 1.83\ RPM1400 - 0.43\ WS20 + 1.10\ WS40 - 0.67\ WS80 \end{aligned}$$

Regression Equation for Percentage Elongation is

$$\begin{aligned} \%\ Elongation = {} & 22.696 + 0.059\ PC - 0.696\ PS + 0.637\ PT - 0.163\ SPR3 \\ & + 0.104\ SPR4 + 0.059\ SPR5 - 0.296\ RPM355 - 0.385\ RPM710 \\ & + 0.681\ RPM1400 + 0.237\ WS20 - 0.074\ WS40 - 0.163\ WS80 \end{aligned}$$

The residual diagnostic plots presented in Figs. 6, 7 and 8 confirm the statistical adequacy of the developed GLM models for UTS, YS, and percentage elongation. In all cases, the normal probability plots show residuals distributed closely along the reference line, indicating that the assumption of normality is satisfied. The residuals versus fitted values plots exhibit random dispersion without noticeable patterns, confirming constant variance and homoscedasticity across predicted values.

The histograms of residuals are approximately symmetric and centered around zero, further supporting the normal distribution of errors. In addition, the residuals versus order plots do not show any systematic trends or cyclic behavior, indicating

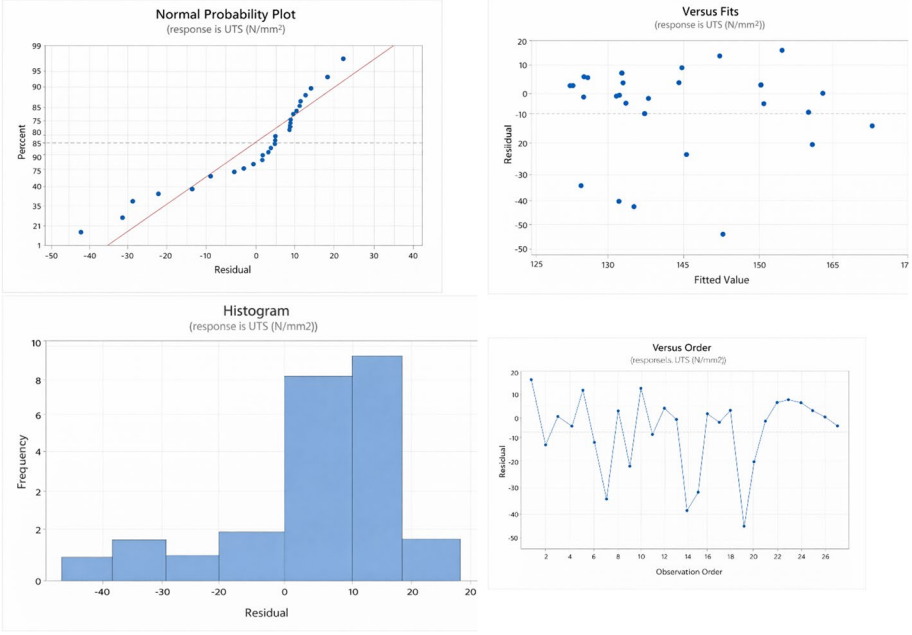

Fig. 6 Graphs for normal probability plot, residuals vs. fits, histogram of residuals, residuals vs. order for UTS (Using Minitab®)

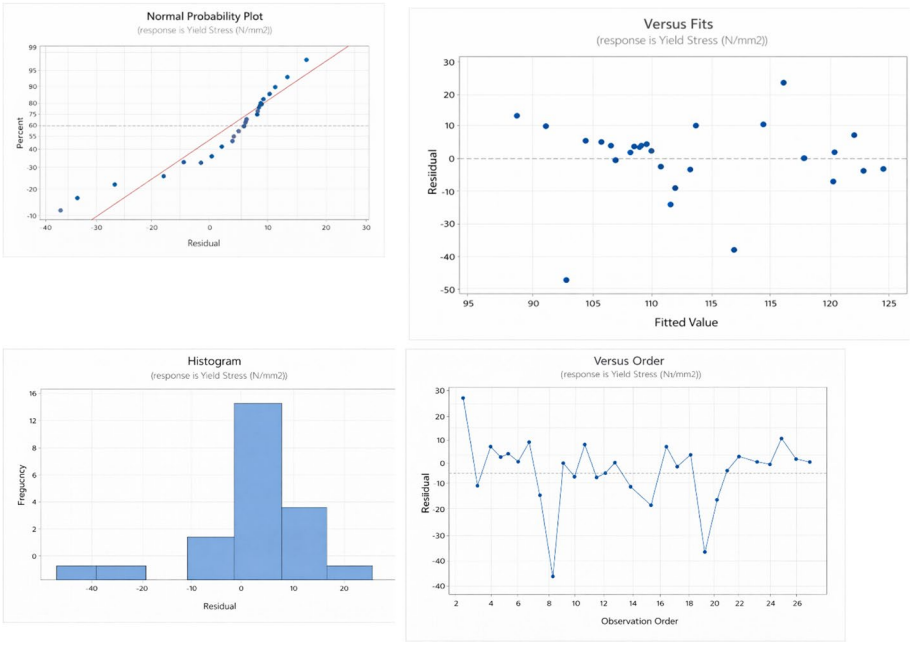

Fig. 7 Graphs for normal probability plot, residuals vs. fits, histogram of residuals, residuals vs. order for YS (Using Minitab®)

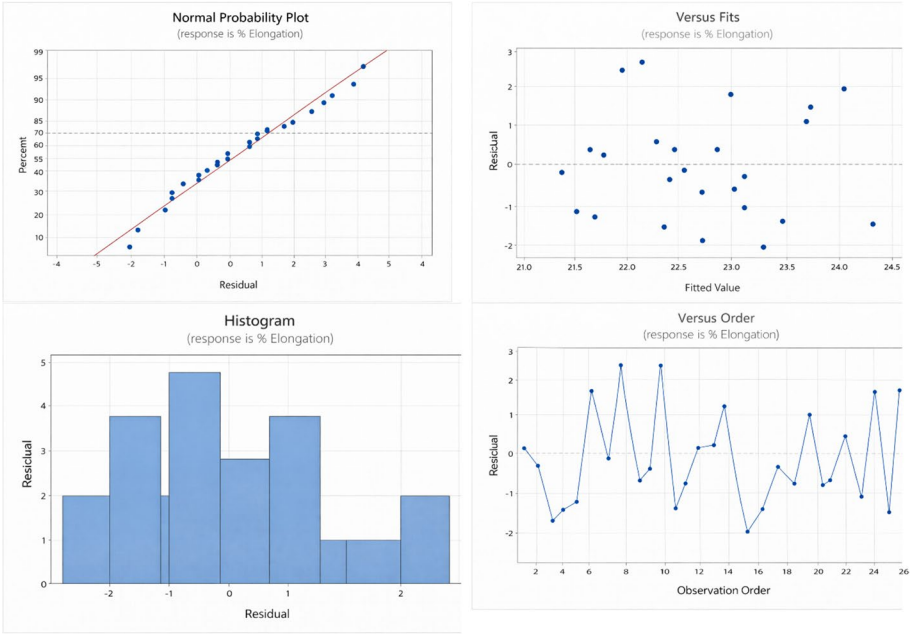

Fig. 8 Graphs for normal probability plot, residuals vs. fits, histogram of residuals, residuals vs. order for % elongation (Using Minitab®)

independence of observations and absence of sequence-related bias. Although slightly higher variation is observed for percentage elongation compared to strength responses, the residuals remain within acceptable statistical limits. Overall, the diagnostic plots validate the adequacy, reliability, and predictive capability of the developed ANOVA–GLM models within the investigated experimental range.

Confirmation of regression model

The adequacy and predictive capability of the developed regression models were validated by comparing experimental and predicted values of ultimate tensile strength (UTS), yield strength (YS), and percentage elongation, as presented in Table 7. For UTS, most prediction errors fall within ± 10%, indicating good agreement between experimental and predicted values. The percentage error ranges from − 12.15% to + 13.19% for most trials, with a maximum deviation of 23.31% observed in Run 15. Except for this isolated case, the predicted values follow the experimental trend, confirming that the model effectively captures the influence of process parameters on tensile strength.

Similarly, the yield strength model demonstrates acceptable predictive accuracy, with most errors within ± 10% and a maximum deviation of 15.12%. The close agreement between experimental and predicted YS values confirms the reliability of the GLM model and supports the ANOVA results, which identify the shoulder-to-pin diameter ratio as the dominant parameter.

For percentage elongation, prediction errors are generally within ± 8%, with a few values approaching 10%. The slightly higher variation in elongation is expected due to the greater sensitivity of ductility measurements to experimental variability. Overall, the relatively low prediction errors for all responses confirm that the regression equations provide reliable predictive capability within the investigated parameter range.

Table 7 Comparison of experimental and regression-predicted values of UTS, YS, and % elongation along with percentage error

Run	UTS (MPa) Expt	UTS (MPa) Pred	% Error UTS	Exp YS	Pred YS	% Error	% E	% E	% Error % E
1	174.37	153.19	−12.15	139.07	116.05	−16.55	22	21.778	1.01
2	161.34	165.58	2.63	121.27	124.41	2.59	21.2	21.378	0.84
3	163.95	158.84	−3.12	129.05	121.97	−5.49	20.8	22.355	7.48
4	137.82	134.79	−2.20	107.37	103.59	−3.52	20.4	21.689	6.32
5	153.33	139.53	−9.00	118.65	108.65	−8.43	20.4	21.511	5.45
6	132.25	134.38	1.61	104.72	108.22	3.34	24.8	22.977	7.35
7	101.63	110.23	8.46	60.98	62.36	2.26	22	21.645	1.61
8	147.78	139.19	−5.81	106.91	104.85	−1.93	24.4	21.956	10.02
9	126.01	140.1	11.18	103.2	105.71	2.43	22	22.711	3.23
10	162.25	144.56	−10.90	124.6	114.33	−8.24	22.4	22.533	0.59
11	156.84	156.95	0.07	118.7	122.69	3.36	24.8	22.133	10.75
12	159.78	150.21	−5.99	122	120.25	−1.43	22	23.11	5.05
13	130.5	126.16	−3.33	101.26	101.87	0.6	22.8	22.444	1.56
14	101.59	111.63	9.89	97.96	106.93	9.16	22.8	22.266	2.34
15	101.98	125.75	23.31	92.51	106.5	15.12	25.2	23.732	5.83
16	132.25	124.22	−6.06	105.8	96.06	−9.21	22	22.4	1.82
17	135.08	139.6	3.35	104.94	103.13	−1.72	20.8	22.022	9.19
18	140.49	149.51	6.42	108.02	103.99	−3.73	22	22.711	6.66
19	102.88	116.45	13.19	83.93	89.75	6.93	22.8	23.311	1.36
20	146.74	157.3	7.21	113.2	120.22	6.2	22	22.889	3.23
21	154.02	150.46	−2.23	117.75	117.78	0.03	24.8	24	4.48
22	137.26	147.98	7.82	105.02	99.4	−5.35	22.4	23.311	2.78
23	143.59	148.92	8.58	108.78	104.46	−3.97	23.2	22.889	1.53
24	137.11	148.1	8.02	107.42	104.03	−3.16	22.8	24.356	6.62
25	132.87	141.14	6.22	106.51	93.59	−12.13	24.8	23.689	7.35
26	135.92	140.9	3.67	105.6	100.66	−4.68	21.2	23.156	9.85
27	133.72	135.6	1.41	105.37	101.52	−3.65	26	23.044	7.52

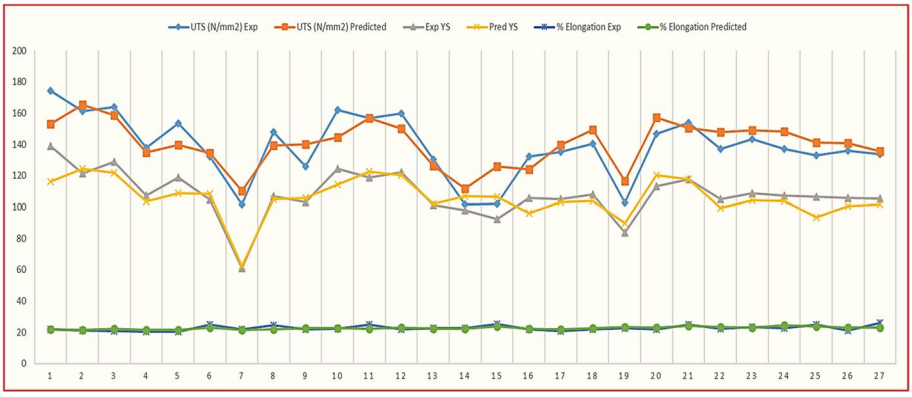

Fig. 9 Comparison of experimental and predicted mechanical properties (UTS, YS, and % Elongation) for 27 FSW AA3103 welded specimens

These results validate the robustness of the developed models and their suitability for process optimization of friction stir welded AA3103 joints.

Figure 9 presents the comparison between experimental and predicted values of UTS, YS, and percentage elongation for all 27 experimental runs. The predicted curves closely follow the experimental trends for both UTS and YS, indicating good agreement and consistent model performance. Minor deviations are observed at a few runs, particularly around Runs 7, 15, and 19; however, the overall alignment confirms that the regression model effectively captures the dominant influence of process parameters. The strength responses also show similar peak and minimum positions in both experimental and predicted datasets, demonstrating reliable predictive capability across different parameter combinations.

Conclusions

The present investigation systematically evaluated the influence of tool pin profile, shoulder-to-pin diameter ratio (D/d), rotational speed, and welding speed on the tensile performance of friction stir welded AA3103 aluminium alloy using a structured Taguchi L9 experimental design executed three times. Based on experimental results, Signal-to-Noise ratio analysis, ANOVA, and regression modeling, the following conclusions are drawn:

i. Dominant Parameter for Strength:
Statistical analysis confirmed that the shoulder-to-pin diameter ratio (D/d) is the only parameter that significantly influences both ultimate tensile strength (UTS) and yield strength (YS) at the 95% confidence level. ANOVA results yielded p-values of 0.030 for UTS and 0.039 for YS, identifying D/d as the primary governing factor for strength development.

ii. Optimal Strength Condition:
The maximum UTS of 174.37 MPa and corresponding YS of 139.07 MPa were obtained at D/d = 3 using the square pin profile. This indicates that a lower shoulder diameter relative to pin diameter improves mechanical performance within the investigated parameter range.

iii. Effect of Tool Geometry on Ductility:

Percentage elongation was statistically insensitive to individual parameter dominance; however, S/N ratio analysis indicated that tool pin profile has a relatively greater influence on ductility. The triangular pin profile exhibited improved elongation performance, with a maximum value of 26%.

iv. Secondary Influence of Speed Parameters:

Rotational speed showed moderate influence on both strength and ductility, whereas welding speed exhibited minimal statistical contribution within the selected experimental range. These results indicate that geometric parameters have a greater effect on tensile performance than speed variations.

v. Model Adequacy and Predictive Capability:

Residual diagnostic plots confirmed normality, homoscedasticity, and independence of errors, validating the GLM assumptions. Most prediction errors for UTS and YS were within ± 10%, indicating reliable predictive capability of the regression models. Although slightly higher variation was observed for elongation, the models adequately captured overall response trends.

vi. Process Optimization Insight:

Multi-response evaluation indicates that strength optimization favors a lower D/d ratio combined with moderate rotational speed, while ductility improvement is influenced more by non-cylindrical pin geometries. The statistical hierarchy established through S/N and ANOVA analysis provides a clear guideline for parameter selection based on performance requirements.

The present study demonstrates that a statistically structured experimental design combined with GLM-based modeling effectively quantifies parameter influence in friction stir welding of AA3103 alloy. The findings provide a practical guideline for optimizing AA3103 joints in sheet-based industrial applications. The developed regression equations can be used as predictive tools within the investigated parameter range; however, extrapolation beyond this range should be approached cautiously. Future work may extend the parameter window or incorporate multi-objective optimization techniques to further improve joint performance reliability.

Nomenclature

AA Aluminium Alloy
AA3103 Aluminium–Manganese Alloy (3xxx Series)
ANOVA Analysis of Variance
ASTM American Society for Testing and Materials
D/d Shoulder-to-Pin Diameter Ratio
DF Degrees of Freedom
DOE Design of Experiments
Exp Experimental
FSW Friction Stir Welding
GLM General Linear Model
L9 Taguchi Orthogonal Array
MPa Mega Pascal
MS Mean Square
PC Pin Circular
PS Pin Square

PT Pin Triangular
Pred Predicted
RPM Revolutions Per Minute
S/N Signal-to-Noise Ratio
SPR Shoulder-to-Pin Ratio
SS Sum of Squares
UTM Universal Testing Machine
UTS Ultimate Tensile Strength
WS Welding Speed
YS Yield Strength
%E Percentage Elongation

Supplementary Information

The online version contains supplementary material available at https://doi.org/10.1186/s44147-026-01028-0.

Supplementary Material 1.

Acknowledgements
The authors would like to thank their institution for providing laboratory facilities and technical support for conducting this research work.

Authors' contributions
Ganesh Jagannath Pagar (Corresponding Author) conceived the research work, conducted the experiments, performed statistical analysis and prepared the manuscript. Ganjanan N Shelke contributed to experimental planning, data interpretation, technical guidance, and manuscript review. Both authors read and approved the final manuscript.

Funding
The authors received no financial support from any funding agency, organization, or institution for this research work.

Data availability
The datasets generated and analyzed during the current study are available from the corresponding author, Ganesh Jagannath Pagar, on reasonable request.

Declarations

Competing interests
The authors declare that they have no competing interests.

Received: 27 February 2026 / Accepted: 22 April 2026
Published online: 02 May 2026

References

1. Kilic S, Ezgimen AA, Taban E (2025) A comprehensive literature review on friction stir welding: Process parameters, joint integrity, and mechanical properties. J Eng Res 123(5):1–21. https://doi.org/10.1016/j.jer.2023.09.005
2. Di Bella G (2023) Effect of process parameters on friction stir welded joints: A detailed review. Metals 13(7):1176. https://doi.org/10.3390/metals13071176
3. Choi JW (2025) Critical review of solid-state welding for aluminium alloys with high performance: FSW and beyond. J Mater Res 67(4):211–230. https://doi.org/10.1007/s12540-025-02007-5
4. El-Sayed AY, Shash MA, Rabou, Mahmoud G, El-Sherbiny (2021) Welding and processing of metallic materials by using friction stir technique: a review. J Adv Join Process. Elsevier
5. El-Moayed H, Shash AY, Rabou MA, Mahmoud G, El-Sherbiny (2020) A detailed process design for conventional friction stir welding of aluminium alloys and an overview of related knowledge, engineering reports. Published by Wiley
6. El-Moayed MH, Shash AY, Rabou MA, Mahmoud G, El-Sherbiny (2021) A coupled statistical and numerical analysis of the residual properties of AA6063 friction stir welds. J Adv Join Process. Elsevier. Accepted 19th of Jan
7. El-Sayed MM, Shash AY, Abd-Rabou M (2017) Finite Element Modeling of Aluminum Alloy AA5083-O Friction Stir Welding Process. J Mater Process Technol 252:13–24
8. Mostafa El-Sayed AY, Shash, Tamer S, Mahmoud, Abd Rabou M (2018) Effect of Friction Stir Welding Parameters on the Peak Temperature and the Mechanical Properties of Aluminum Alloy 5083-O Improved Performance of Materials, Edition: 1, Chapter: 2, Publisher: Advanced Structured Materials, vol 72. Springer, Cham, Editors: Andreas Öchsner, Holm Altenbach, pp.11–25
9. El-Sayed MM, Shash AY, Abd-Rabou M (2017) "Heat transfer simulation and effect of tool pin profile and rotational speed on mechanical properties of friction stir welded AA5083-O". Journal of Welding and Joining (in press). Accepted 14 of March

10. El-Sayed MM, Shash AY, Abd-Rabou M (2017) Influence of the Welding Speeds and Changing the Tool Pin Profiles on the Friction Stir Welded AA5083-O Joints, Journal of Welding and Joining, in press, accepted 21 of March
11. Gokulachandran J (2025) Reliability assessment and optimization of FSW joints in aluminium alloys using advanced statistical modeling. Sci Rep 15:33297. https://doi.org/10.1038/s41598-025-04694-X
12. El-Moayed M, Shash AY, Rabou MA, Mahmoud G, El-Sherbiny (2021) Thermal-induced Residual Stresses and Distortions in Friction Stir Welds - A Literature Review, Journal of Welding and Joining, The Korean Welding and Joining Society, Accepted 3rd of June
13. George G, Yacout, Ahmed Y, Shash, Hesham Hegazi, El-Sherbiny M (2025) Application of response surface methodology for optimizing friction stir welding parameters of AA6082-T6 aluminium alloy, Accepted 8 July 2025, Available online 9 July 2025, Journal of Materials Research and Technology, publisher Elsevier
14. Yacout GG, Shash AY, Hegazi HA et al (2025) Comparative experimental and statistical study of conventional and bobbin tool friction stir welding of AA6061-T6 aluminum alloy. J Eng Appl Sci 72:255. https://doi.org/10.1186/s44147-025-00834-2
15. Mishra RS, Ma ZY (2018) Friction stir welding and processing. Mater Sci Eng R Rep 50(1–2):1–78. https://doi.org/10.1016/S0927-796X(00)00035-6
16. Sahu PK, Pal S, Bhowmick S (2020) Effect of clamping and fixture rigidity on friction stir welding of aluminium alloys. J Manuf Process 57:1–10. https://doi.org/10.1016/j.jmapro.2020.06.012
17. Patel V, Li WY, Vairis A (2021) Influence of process parameters on surface morphology and mechanical properties of friction stir welded aluminium alloys. J Mater Res Technol 14:2143–2154. https://doi.org/10.1016/j.jmrt.2021.07.065
18. Davis JR (2018) Aluminium and Aluminium Alloys. ASM International, Materials Park, OH
19. Kumar A, Singh R, Patel V (2021) Mechanical and corrosion behaviour of 3xxx series aluminium alloys: A review. J Mater Res Technol 15:3201–3215. https://doi.org/10.1016/j.jmrt.2021.09.032
20. Sharma C, Dwivedi DK, Kumar P (2019) Effect of process parameters on friction stir welding of aluminium alloys: A review. J Mater Res Technol 8(6):5493–5514. https://doi.org/10.1016/j.jmrt.2019.09.003
21. Singh R, Kumar A, Choudhary S (2020) Tool material selection and wear behaviour in friction stir welding of aluminium alloys. J Manuf Process 52:157–170. https://doi.org/10.1016/j.jmapro.2020.01.028
22. Rajakumar S, Muralidharan C, Balasubramanian V (2019) Tool wear and thermal stability of H13 steel during friction stir welding of aluminium alloys. Trans Nonferrous Met Soc China 29(6):1125–1136. https://doi.org/10.1016/S1003-6326(19)65032-4
23. Palanivel R, Mathews PK, Murugan N (2021) Influence of tool pin profile on microstructure and mechanical properties of friction stir welded aluminium alloys. J Mater Res Technol 14:289–302. https://doi.org/10.1016/j.jmrt.2021.06.041
24. Elangovan K, Balasubramanian V (2018) Effect of tool geometry and shoulder diameter on the formation and mechanical behaviour of friction stir welded aluminium joints. Mater Des 30(9):3363–3371. https://doi.org/10.1016/j.matdes.2009.04.028
25. Kumar N, Singh R, Sharma C (2020) Effect of rotational and traverse speed on weld quality in friction stir welding of aluminium alloys. J Manuf Process 58:748–759. https://doi.org/10.1016/j.jmapro.2020.08.042
26. Antony J (2019) Design of experiments for engineers and scientists: A systematic approach to process optimization. Qual Eng 31(2):241–252. https://doi.org/10.1080/08982112.2018.1544615
27. Ross PJ (2018) Taguchi techniques for quality engineering. McGraw-Hill Education, New York
28. Montgomery DC (2019) Design and analysis of experiments. Wiley, Hoboken
29. Gokulachandran J (2022) Statistical modelling and optimization of friction stir welding process parameters. Mater Today Proc 62:1420–1426. https://doi.org/10.1016/j.matpr.2022.02.186
30. Verma S, Kumar A, Singh R (2021) Multi-response optimization in friction stir welding of aluminium alloys. J Manuf Process 64:1124–1135. https://doi.org/10.1016/j.jmapro.2021.02.031
31. Rao PS, Reddy GM (2020) Analysis of variance and regression modelling for friction stir welded aluminium joints. Trans Nonferrous Met Soc China 30(5):1245–1256. https://doi.org/10.1016/S1003-6326(20)65260-7
32. Elangovan K, Balasubramanian V (2018) Influences of tool pin profile and welding speed on the formation of friction stir processed zone in AA2219 aluminium alloy. Mater Des 30(7):188–198. https://doi.org/10.1016/j.matdes.2008.04.034
33. Rajakumar S, Muralidharan C, Balasubramanian V (2018) Influence of friction stir welding process and tool parameters on strength properties of AA7075 aluminium alloy joints. Mater Des 32(2):535–549. https://doi.org/10.1016/j.matdes.2010.08.025
34. Palanivel R, Mathews PK, Murugan N (2019) Effect of tool rotational speed and pin profile on microstructure and tensile strength of friction stir welded AA5083 alloy. Mater Des 40:7–16. https://doi.org/10.1016/j.matdes.2012.03.025
35. Kumar K, Kailas SV (2018) On the role of axial load and tool geometry in friction stir welding of aluminium alloys. Mater Manuf Process 23(4):1–8. https://doi.org/10.1080/10426910802033479
36. Cavaliere P, Squillace A, Panella F (2018) Effect of welding parameters on mechanical and microstructural properties of friction stir welded AA6082 joints. J Mater Process Technol 200(1–3):364–372. https://doi.org/10.1016/j.jmatprotec.2007.09.030
37. Lorrain O, Favier V, Zahrouni H, Lawrjaniec D (2018) Understanding the material flow path of friction stir welding process using advanced modelling techniques. J Mater Process Technol 186(1–3):131–137. https://doi.org/10.1016/j.jmatprotec.2006.12.018
38. Tuneer S, Kumar A (2020) Effect of tool geometry on mechanical properties of friction stir welded aluminium alloys: A comparative study. J Mater Eng Perform 29(4):2254–2265. https://doi.org/10.1007/s11665-020-04612-3
39. Sharma C, Dwivedi DK, Kumar P (2020) Effect of shoulder diameter to pin diameter ratio on mechanical properties of friction stir welded joints. J Manuf Process 45:101–110. https://doi.org/10.1016/j.jmapro.2019.06.021
40. Verma S, Kumar A, Singh R (2021) Taguchi based optimization of friction stir welding parameters for improving tensile strength of aluminium alloy joints. J Manuf Process 64:1124–1135. https://doi.org/10.1016/j.jmapro.2021.02.031
41. Rao PS, Reddy GM (2020) Multi-response optimization and regression modelling of friction stir welded aluminium joints using ANOVA approach. Trans Nonferrous Met Soc China 30(5):1245–1256. https://doi.org/10.1016/S1003-6326(20)65260-7

Publisher's note